Fish and Shellfish Immunology 89 (2019) 477–485

Contents lists available at ScienceDirect

Fish and Shellfish Immunology

journal homepage: www.elsevier.com/locate/fsi

Full length article

Edwardsiella tarda-induced miR-7a functions as a suppressor in PI3K/AKT/GSK3β signaling pathway by targeting insulin receptor substrate-2 (*IRS2a* and *IRS2b*) in *Paralichthys olivaceus*

Yuezhong Liu[a], Yuxiang Liu[a], Miao Han[a], Xinxin Du[a,c], Xiumei Liu[a,d], Quanqi Zhang[a,b], Jinxiang Liu[a,b,*]

[a] Key Laboratory of Marine Genetics and Breeding, Ministry of Education, Ocean University of China, Qingdao, 266003, China
[b] Laboratory for Marine Fisheries Science and Food Production Processes, Qingdao National Laboratory for Marine Science and Technology, Qingdao, 266237, China
[c] Department of Life Science and Engineering, Jining University, Jining, China
[d] College of Life Sciences, Yantai University, Yantai, 264005, China

ARTICLE INFO

Keywords:
Paralichthys olivaceus
Edwardsiella tarda
High-throughput sequencing
miR-7a
IRS2
PI3K/AKT/GSK3β pathway

ABSTRACT

To study the effect of *Edwardsiella tarda* infection on miRNAs expression profile in Japanese flounder, fish were injected intraperitoneally with *E. tarda*. The miRNAs involved in regulating immune responses were analyzed by high-throughput sequencing. A total of 164 mature miRNAs were identified, of which 17 miRNAs were differentially expressed (DE miRNAs) after *E. tarda* infection, indicating that they were immune-related miRNAs. To further examine the relationship between the miRNAs and their predicted target mRNAs, a total of 22 predicted target mRNAs, mainly related to endocytic signaling pathway, NF-κB signaling pathway, and p53 signaling pathway, were detected with miRNA mimics in HEK-293T cells by dual-luciferase reporter experiments. Finally, we confirmed that insulin receptor substrate-2 (*IRS2a* and *IRS2b*) were regulated by miR-7a. And the target sites of the 3' untranslated region (UTR) of *IRS2a* and *IRS2b* were verified by dual-luciferase reporter experiments. Furthermore, we found that the *E. tarda* and LPS significantly increased host miR-7a expression. *In vivo* and *in vitro* studies revealed that IRS2-mediated PI3K/AKT/GSK3β signaling pathway was suppressed. Taken together, these results implied that miR-7a might be a key regulator of PI3K/AKT/GSK3β signaling pathway via suppressing the *IRS2a* and *IRS2b* genes.

1. Introduction

Japanese flounder is an important economic aquaculture species which has been widely cultured in China, Korea, and Japan. Intensive culture of Japanese flounder has brought high production and great benefits for the aquaculture farmers. Recently, a great number of reports have given rise to the awareness of the severe economic damages caused by bacterial and viral pathogen infections such as *Edwardsiella tarda*, Vibriosis, and Viral hemorrhagic septicemia virus (VHSV) [1,2]. *E. tarda*, a Gram-negative bacterium, is one of the serious fish pathogens affecting more than 20 species of freshwater and marine fishes including carp, tilapia, eel, catfish, mullet, salmon, trout, turbot, and Japanese flounder [3–5].

MicoRNAs are endogenous small non-coding RNA molecules with approximately 22 nucleotides (nt) in length. miRNAs post-transcriptionally down-regulate gene expression in animals and plants mostly by binding to the 3′ untranslated regions (3′UTRs) of target mRNAs [6]. Reports indicate that miRNAs play a key role in numerous cellular and biological processes such as development, cell differentiation, apoptosis, and immune response [7–9]. Especially, miRNAs have been proved to be closely related to immune response during *E. tarda* infection. In Japanese flounder, miR-194a serves as a target for *E. tarda* to manipulate and escape host immune defense by suppresses type I interferon [10]. In tongue sole, miRNAs are not only important regulators in host defense but may also serve as targets for *E. tarda* manipulation of the host defense system [11]. In addition, accumulating evidences have indicated a diverse regulatory role of miRNAs during pathogen infection in teleost. For example, miR-145-5p is involved in the RLR signaling pathway in miiuy croaker via targeting *MDA5* after poly(I:C) stimulation [12]. Megalocytivirus induced miR-731 in Japanese flounder can facilitate viral infection by suppressing *IRF7* and cellular tumor antigen *p53* [13]. In teleost, miR-21 can inhibit the

* Corresponding author. Key Laboratory of Marine Genetics and Breeding, Ministry of Education, Ocean University of China, 266003, Qingdao, Shandong, China.
E-mail address: liujinxiang@ouc.edu.cn (J. Liu).

https://doi.org/10.1016/j.fsi.2019.03.076
Received 25 February 2019; Received in revised form 29 March 2019; Accepted 29 March 2019
Available online 30 March 2019

expression of cytokines by targeting *TLR28*, thereby inhibiting the generation of excessive immunity and maintaining the balance of the body [14]. In orange spotted grouper, miR-146a promotes red spotted grouper nervous necrosis virus by supressing *TRAF6* [15]. However, studies on the regulatory relations between miRNA and immune signaling pathways in teleost are still limited compared with studies about the immune-related genes.

In the present study, we focused on the role of miRNAs in the interactions between host and pathogen in order to provide a new investigation to the process of disease outbreak in the commercially cultured Japanese flounder stocks. To date, the immunoregulatory mechanisms of miRNAs in Japanese flounder diseases remain largely unclear. With the development of next-generation sequencing technologies, RNA sequencing has become an efficient approach to profile the transcriptomes at the unprecedented depth of coverage and a lower cost. Therefore, dissecting the biological functions of miRNAs by deep sequencing may help us understand the response to bacterial infection in Japanese flounder liver and gain insights into the systemic response of fish to bacterial infection. In this study, we found that *E. tarda* and LPS significantly upregulated the expression of miR-7a in Japanese flounder. And *IRS2a* and *IRS2b* were shown to be target genes of miR-7a, which was confirmed by dual-luciferase reporter experiments. In summary, our studies suggested that miR-7a might be a suppressor in PI3K/AKT/GSK3β signaling pathway by targeting *IRS2a* and *IRS2b* in Japanese flounder, which provided more information about the functions of miRNA on regulating immune response in teleost.

2. Materials and methods

2.1. Ethics statement

Japanese flounder samples were collected from Haiyang Yellow Sea Aquatic Product CO., Ltd, Shandong, China. All the experiments were conducted according to the Guidelines for the Institutional Animal Care and Use Committee of the Ocean University of China.

2.2. Experimental fish and bacteria

A total of 30 healthy 1-year-old Japanese flounder of nearly uniform size (average body length 16.3 cm; average weight 70.5 g) were collected and acclimated at 19 °C in aerated circulating seawater without feeding for one week. Fish were confirmed to be pathogen-free by primers based on the specific *esaV* gene of pathogenic *E. tarda* as reported previously before challenge [16,17].

The *E. tarda* strain EIB202 used in this study was acquired from the Laboratory of Microbiology, Ocean University of China, and suspended in Ringer's solution for marine teleost to 2×10^7 CFU mL^{-1}.

2.3. Bacterial infection and sample collection

Infection experiment was performed as previously described with modifications [18]. In short, Japanese flounder were assigned to three groups, including bacterial challenge experiment group (EG), Ringer's solution control group (RC), and blank control group (BC). EG and RC groups were injected intraperitoneally with 1 mL E. *tarda* suspension and Ringer's solution, respectively. BC individuals did not receive any treatment.

The liver tissues were collected after 3 and 24 h post injection (hpi) in EG and RC groups. Before experiment (0 h), three fish were randomly selected as BC. Three individuals were randomly selected for RNA extraction at each time point. Finally, a total of 15 samples were obtained. Liver tissues were collected in triplicate from each fish, frozen immediately in liquid nitrogen, and then stored at −80 °C until use.

2.4. RNA preparation, library construction, and sequencing of small RNAs

Total RNA from each sample was extracted from liver tissues using *mir*Vana™ miRNA Isolation Kit (Life Technologies, USA) according to the manufacturer's instructions. The quality and quantity were evaluated via 1.5% agarose gel electrophoresis and spectrophotometry using NanoPhotometer Pearl and Agilent 2100 Bioanalyzer. All library construction and high-throughput sequencing were carried out by Novogene Company (Beijing, China). The libraries were constructed with NEBNext® Multiplex Small RNA Library Prep Set for Illumina® (NEB, USA.) following manufacturer's protocol. Then libraries were sequenced on an Illumina Hiseq 2500 platform and 50 bp single-end reads were generated.

2.5. Data processing and bioinformatics analysis

Raw reads were cleaned by removing adaptors and sequences with low quality. After trimming 3' adaptors with fastx-clipper tool (http://hannonlab.cshl.edu/fastx_toolkit/), clean high-quality sequencing reads were used as the experimental data. The miRNA identification analysis was performed against Japanese flounder reference genome using the miRDeep2 (version 2.0.0.8) software package with default commands [19].

Briefly, clean reads were aligned to the reference genome by mapper module and the miRDeep2 module excised genome sequence (approximately 100 bp) as potential miRNA precursor. For a conservative prediction, we adopted the miRDeep2 score which yielded a signal-to-noise ratio higher than 10:1 as a cut-off threshold. Therefore, all precursors with total miRDeep scores above the threshold were considered as putative miRNAs.

The precursors that provided a significant match to the GenBank noncoding RNA database (http://www.blast.nvbi.nlm.nih.gov/) and Rfam database (http://rfam.sanger.ac.uk/) by BLAST searches were classified as other classes of non-coding RNAs, such as tRNAs, rRNAs, snRNAs, and snoRNAs. The remaining putative miRNAs were further blasted against miRBase database (http://www.mirbase.org/search.shtml). Any precursor that provided a match with an E-value $\leq 1 \times e^{-5}$ to a stem-loop sequences in the database was accepted as an authentic miRNA. The putative miRNAs identified by the miRDeep program that did not show a significant match to miRBase were regarded as novel miRNAs.

2.6. DE miRNAs identification, target genes prediction and functional enrichment analysis

Firstly, read counts of identified miRNAs were normalized by the transcripts per million reads (TPM). DESeq v1.16.0 was used to identify DE miRNAs among the groups. The miRNAs were considered significantly differentially expressed when the expression quantity changes more than 1.5 times. Due to the large individual differences in Japanese flounder, the *p*-value obtained by this method was less than 0.1.

Putative target genes of DE miRNAs were predicted using miRanda (version 3.3a) (http://www.microrna.org/) [20] and RNA22 v2 [21]. The miRanda parameters were set as score > 120 and free energy < −20 kcal/mol. The RNA22 parameters were set according to the default parameters. The results predicted by the two algorithms were combined, and the overlaps were regarded as putative target genes of miRNAs.

The predicted target genes were enriched by GO terms and KEGG categories using DAVID [22].

2.7. Plasmids construction and dual-luciferase reporter assays

The recombined reporter vectors pmirGLO-gene-WT were constructed by inserting 3′UTR region into the pmirGLO-basic vector

between *Sac* I and *Xho* I sites (Supplemental Table S1). The mutant-type vectors pmirGLO-IRS2a-MT and pmirGLO-IRS2b-MT were generated from the pmirGLO-IRS2a-WT and pmirGLO-IRS2b-WT via PCR approach according to the protocol of the QuikChange site-directed mutagenesis kit (Agilent Technologies, Santa Clara, CA, USA).

For the transfection experiment, HEK-293T cells were seeded into 24-well plate. Then the plasmids and synthesized miRNAs were co-transfected into HEK-293T cells by Lipofectamine™ 2000 (Invitrogen, USA) according to the manufacturer's instructions. The sequences of synthesized miRNAs were listed in Table S1. At 48 h post-transfection, the cells were collected for activity determination using by Dual-Luciferase Reporter Assay System (E1910, Promega, USA). Luciferase activity was achieved against the renilla luciferase control. For each experiment, three independent triplicated experiments were conducted.

2.8. Primary liver cell culture, Leukocyte isolation, and LPS stimulation

Liver tissue from half-year-old Japanese flounder was sampled aseptically, placed into Leibovitz's L-15 medium (Invitrogen) and minced into small pieces (about 1 mm^3). Subsequently, the minced tissue was transferred into culture flask containing the complete medium of L-15 supplemented with 20% fetal bovine serum (FBS, Gibco, America), 100 U/mL penicillin, 0.1 mg/ml streptomycin, and 10 mM non-essential amino acids (Gibco, America) at 24 °C. Half of complete medium was replaced every 5 days.

When the cells migrated and formed a confluent monolayer, the old medium was removed and cells was washed twice with PBS, digested with 0.25% trypsin-EDTA solution (Sigma, America) and transferred into a 24-well plate for LPS challenge. The primary liver cells were collected after stimulated with50 μg/mL LPS at 0, 3, 6, 12, and 24 h. The cells were washed with PBS, centrifuged at 800 × *g* for 5 min at 4 °C, and then stored at −80 °C for RNA extraction.

Head kidney lymphocytes (HKLs) was isolated as described before [23], and cultured in L-15 medium. The HKLs were collected after challenged with 50 μg/mL LPS at 0, 3, 6, 12, and 24 h. Then, the HKLs were washed with PBS and stored at −80 °C for RNA extraction.

2.9. RNA extraction and cDNA synthesis

For mRNA analysis, total RNA was extracted separately using Trizol Reagent (Invitrogen, Carlsbad, CA, USA) following the manufacturer's instructions and treated with RNase-free DNase I (TaKaRa, Dalian, China) to eliminate the genomic DNA contamination. cDNA synthesis was performed using Reverse Transcriptase M-MLV Kit (TaKaRa, Dalian, China).

For miRNA analysis, total RNA was extracted by using *mir*Vana™ miRNA Isolation Kit (Life Technologies, USA) and cDNA synthesis was reverse transcribed with Mir-X™ miRNA First-Strand Synthesis Kit (Clontech, Mountain View, CA) following the manufacturer's instructions.

2.10. qRT-PCR for mRNA and miRNA

For mRNA and miRNA expression analysis, qRT-PCR was performed with 2 × SYBR Green qPCR Master Mix (US Everbright Inc.) by LightCycler 480 (Roche, Forrentrasse, Switzerland). The *18S rRNA* and *U6 snRNA* were used as internal reference gene, respectively. Gene-specific primer pairs were listed in Table S1. During qRT-PCR, samples from three individuals were pooled together and performed in triplicate. Relative expression level of miRNA and mRNA was calculated by $2^{-\Delta\Delta Ct}$ method.

The qRT-PCR data were subjected to analysis using one-way ANOVA with SPSS 20.0 (IBM, New York, USA). $P < 0.05$ was considered to indicate statistical significance. All data were expressed as the mean ± standard error of the mean (SEM).

Table 1
Summary of samples sequenced for discovery of flounder immune-related miRNA genes in liver.

Sample	Raw reads	Q30 (%)	Clean reads	Unique reads[a]	Acc# NCBI SRA[b]
BC-1	11233673	96.06	11031006	384757	SRR6853311
BC-2	10614907	97.78	10539301	208385	SRR6853310
BC-3	11897737	94.99	11726037	605788	SRR6853313
EG3-1	13644825	96.42	13488359	331415	SRR6853312
EG3-2	9750131	95.79	9615528	380525	SRR6853307
EG3-3	12611776	95.71	12438501	370912	SRR6853306
RC3-1	10528187	95.58	10310432	446578	SRR6853309
RC3-2	11453599	97.71	11260991	360402	SRR6853308
RC3-3	11246984	95.42	10913016	595550	SRR6853305
EG24-1	12495077	95.84	12210589	323790	SRR6853304
EG24-2	12046632	95.59	11839877	396686	SRR6853318
EG24-3	14757778	96.94	14613849	401562	SRR6853317
RC24-1	13147785	96.76	12959055	342649	SRR6853316
RC24-2	12535057	95.92	12301185	363834	SRR6853315
RC24-3	12733781	95.80	12537982	318608	SRR6853314

[a] Number of unique reads in a sample.
[b] Accession number to sequencing data from each of the samples in NCBI SRA database.

3. Results

3.1. Identification of miRNAs

Samples from five time points each with three replicates (BC-1, BC-2, BC-3, EG3-1, EG3-2, EG3-3, RC3-1, RC3-2, RC3-3, EG24-1, EG24-2, EG24-3, RC24-1, RC24-2, and RC24-3) were analyzed by small RNA sequencing. The concentration of total RNA ranged from 178 to 805 ng/μl (total volume 100 μl). The number of raw reads from each sample ranged from 9750131 to 14757778, while the number of adaptor trimmed and quality filtered reads ranged from 9615528 to 14613849. The raw sequencing data was deposited at the National Center for Biotechnology Information (Accession number SRP135934). After elimination of redundancy, the number of unique reads from each sample ranged from 208385 to 605788. A preliminary result of the small RNA sequencing was given in Table 1. The clean reads length distribution result showed an essential consistency among all the fifteen libraries, only slight differences were observed. Two clear peaks were observed, one ranged from 21 to 22 nt and the other one 24 nt to 32 nt which represents miRNAs and piwi-interacting RNAs (piRNAs), respectively (Fig. 1A).

After miRDeep analysis and BLAST homology searches against the stem-loop sequences in miRbase (see Materials and Methods), a total of 164 mature miRNAs together with 246 putative precursor sequences were identified. An overview of all such evolutionary conserved precursor (mir) sequences identified along with their corresponding mature 5p and 3p sequences was given in Additional file 1.

Several additional putative precursors with miRDeep scores above threshold didn't show homology with any miRNA gene families in miRBase. These putative novel miRNAs were further analyzed by BLAST against Japanese flounder genome. Precursor sequences that showed multiple significant hits against the genome (more than 5 hits with E-values $> 1 \times e^{-5}$) were removed. Because those sequences were considered most likely to be interspersed repeats or long tandem repeats [24]. After removing the sequences that were shown to have homology with other small RNA databases (see Methods), the remained sequences were regarded as novel miRNAs. A total of 193 novel miRNAs with their precursor and mature sequences as well as their genome locations were given in Additional file 2.

3.2. The identification of DE miRNAs

In the present study, 17 unique miRNAs were identified, which displaying significantly altered expression (> 1.5-fold) in comparison

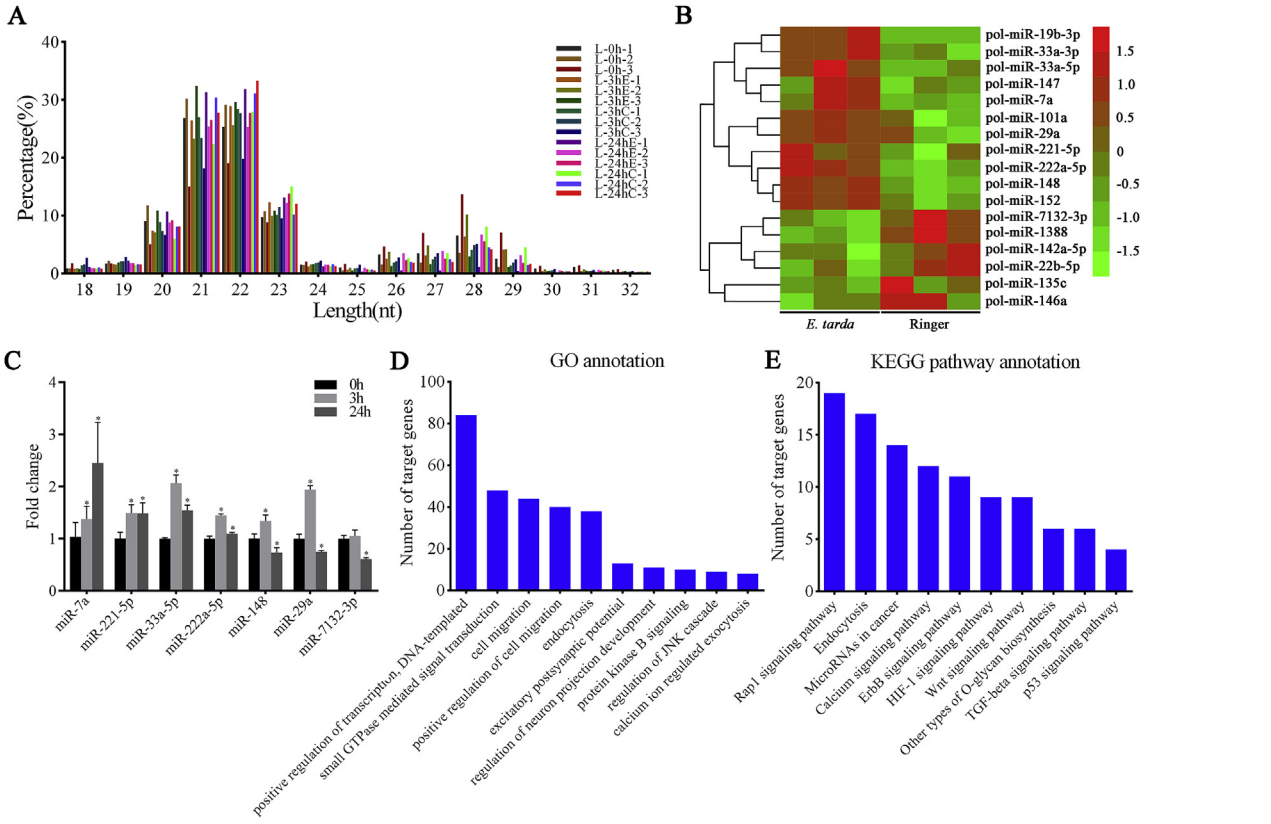

Fig. 1. (A) Length distribution of small RNAs in all groups. The x-axis indicated sequence sizes from 18 nt to 32 nt. The y-axis indicated the percentage of reads for each size. (B) Cluster analysis of differentially expressed miRNAs in Japanese flounder after experimental infection with *E. tarda*. The heat map showed miRNA expression level on a log2 scale, with red and green indicating high and low expression, respectively. (C) Expression profiles of 7 selected miRNAs in liver after *E. tarda* challenge. The miRNA expression level in *E.tarda* treated samples was normalized to that in the control group. Values are shown as mean ± SEM. Asterisks indicated statistical significance ($P < 0.05$). (D) The top ten most enriched GO terms of biological process of the target genes of Japanese flounder. (E) The top ten most enriched KEGG pathways of the target genes of flounder miRNAs. (For interpretation of the references to colour in this figure legend, the reader is referred to the Web version of this article.)

Table 2
Summary of differentially expressed miRNAs. The plus values represent up-regulated fold in the *E. tarda* infection groups, while minus values represent down-regulated fold.

Time post infection	MiRNAs	log2(fold change)	*p*-value
3 h	*pol*-miR-147	+0.92	2.93E-02
	pol -miR-19b-3p	+0.72	2.94E-02
	pol -miR-142a-5p	−0.88	6.63E-02
	pol -miR-22b-5p	−0.89	5.38E-02
24 h	*pol* -miR-33a-3p	+1.49	4.54E-02
	pol -miR-33a-5p	+1.38	3.46E-02
	pol -miR-7a	+1.07	8.31E-04
	pol -miR-101a	+1.03	7.83E-03
	pol -miR-221-5p	+0.93	6.71E-02
	pol -miR-148	+0.87	7.38E-03
	pol -miR-29a	+0.84	8.44E-02
	pol -miR-222a-5p	+0.73	2.42E-02
	pol -miR-152	+0.71	3.09E-02
	pol -miR-7132-3p	−0.57	2.26E-02
	pol -miR-146a	−0.76	7.52E-02
	pol -miR-135c	−0.95	1.75E-02
	pol -miR-1388	−1.33	1.60E-02

between the EG and RC groups (Table 2). At 3 hpi, miR-147 and miR-19b-3p were upregulated, while miR-142a-5p and miR-22b-5p were downregulated. At 24 hpi, nine miRNAs (miR-33a-3p, miR-33a-5p, miR-7a, miR-101a, miR-221-5p, miR-148, miR-29a, miR-222a-5p, and miR-152) were upregulated, while four miRNAs (miR-7132-3p, miR-146a, miR-135c, and miR-1388) were downregulated. A heat map was generated to show the temporal change of DE miRNAs at different time points after *E. tarda* infection (Fig. 1B).

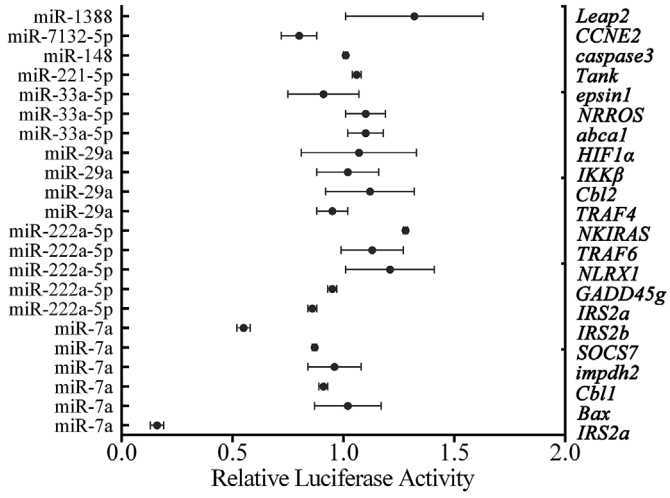

Fig. 2. Validation of selected miRNAs and their target mRNAs. HEK293T cells were co-transfected with different miRNA mimics and their target mRNA-3′UTR reporter plasmids. Relative luciferase activity was measured at 48 h after transfection. For each experiment, three independent triplicated experiments were conducted. Values were shown as means ± SD.

To confirm the differential expression of miRNAs, seven miRNAs were selected and further verified by qRT-PCR. The data showed similar

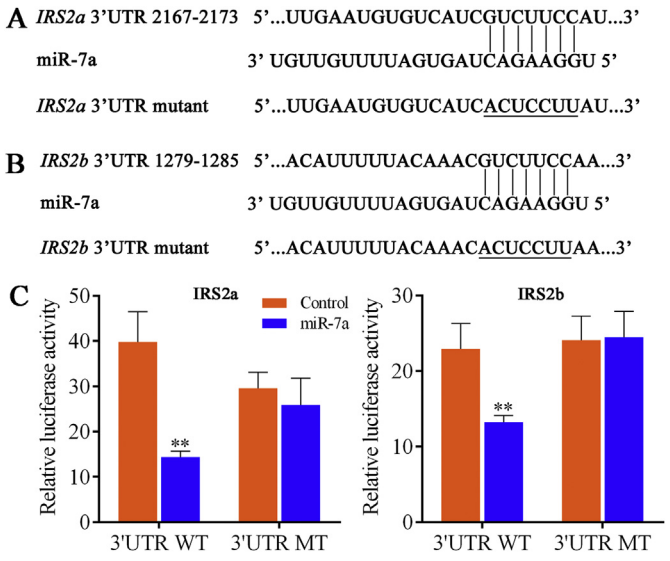

Fig. 3. Japanese flounder *IRS2a* and *IRS2b* are novel targets of miR-7a. (A) Schematic diagram of the predicted target sites of miR-7a in 3′ UTR of *IRS2a*. (B) Schematic diagram of the predicted target sites of miR-7a in 3′ UTR of *IRS2b*. (C) Relative luciferase activities of *IRS2*(s) 3′UTR reporter or mutated *IRS2*(s) 3′ UTR reporter in HEK293T cells with miR-7a mimic or control. Luciferase activity was normalized to renilla luciferase activity. Data are presented as the means ± SD from three independent triplicated experiments. **, $P < 0.01$ versus the controls.

patterns to the results obtained from high throughput sequencing, except miR-148 and miR-29a (Fig. 1C).

3.3. Immune-related miRNA target genes and functional enrichment analysis

Totally 2100 potential target genes of the 17 immune-related DE miRNAs were obtained using the miRanda and RNA22 target gene prediction softwares. Because miRNA regulates different biological processes by targeting diverse genes, these target genes were subjected to GO and KEGG pathway enrichment analysis. A total of 171 GO terms were obtained and classified into three categories, including 82 terms for biological processes, 28 terms for cellular components, and 61 terms for molecular functions. The top ten enriched GO terms for biological processes were associated with calcium ion regulated exocytosis, regulation of JNK cascade, protein kinase B signaling, regulation of neuron projection development, excitatory postsynaptic potential, endocytosis, positive regulation of cell migration, cell migration, small GTPase mediated signal transduction, positive regulation of transcription, and DNA-templated (Fig. 1D). KEGG enrichment analysis obtained 32 pathways. The top ten enriched pathways were involved in p53 signaling pathway, TGF-beta signaling pathway, Other types of O-glycan biosynthesis, Wnt signaling pathway, HIF-1 signaling pathway, ErbB signaling pathway, Calcium signaling pathway, MicroRNAs in cancer, Endocytosis, and Rap1 signaling pathway (Fig. 1E).

3.4. Screening for negative regulatory relationship between miRNAs and mRNAs

It is well known that miRNAs negatively regulate the expression of their target mRNAs. To examine whether there was a negative

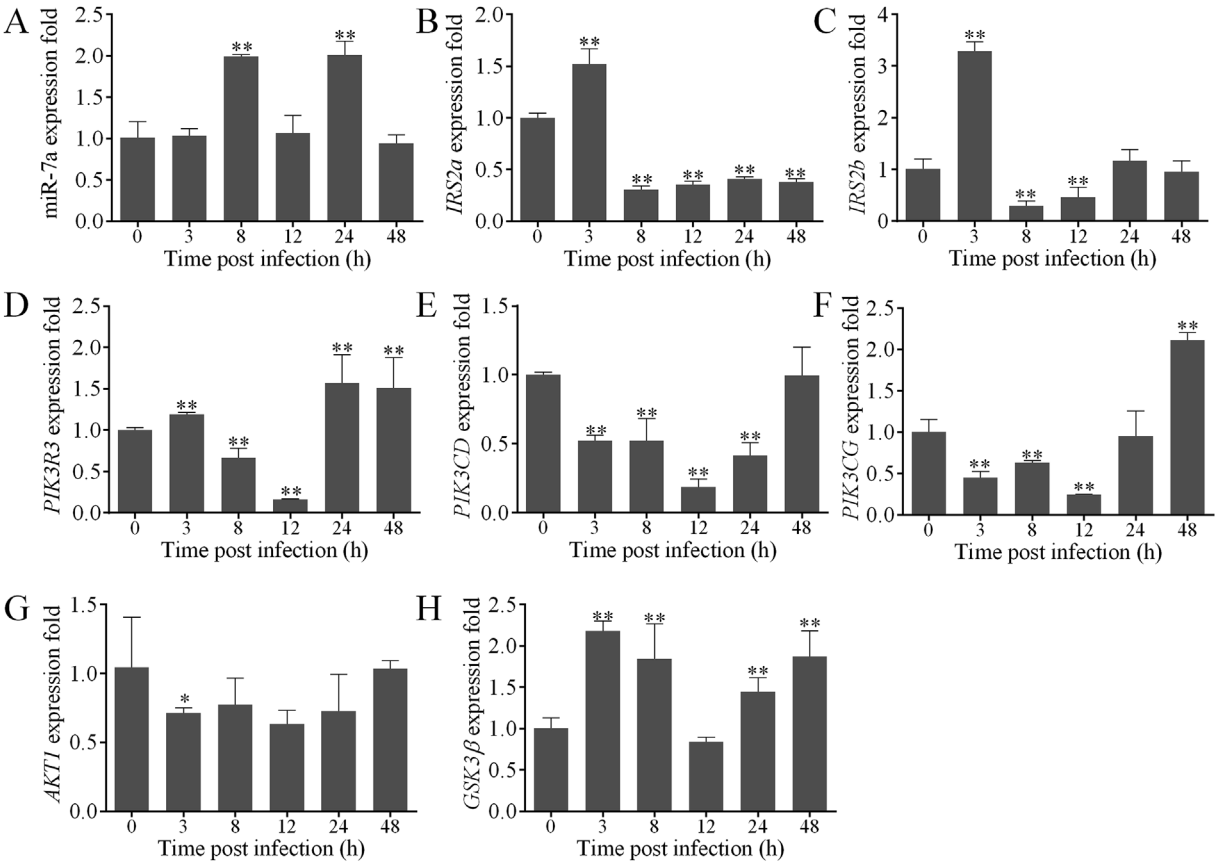

Fig. 4. Upregulated miR-7a inhibits IRS2(s)-mediated PI3K/AKT/GSK3β signaling upon *E. tarda* infected liver. The expression profiles of (A) miR-7a, (B) *IRS2a*, (C) *IRS2b*, (D) *PIK3R3*, (E) *PIK3CD*, (F) *PIK3CG*, (G) *AKT1*, and (H) *GSK3β* at various times post-infection. **, $P < 0.01$; *, $P < 0.05$ versus the controls.

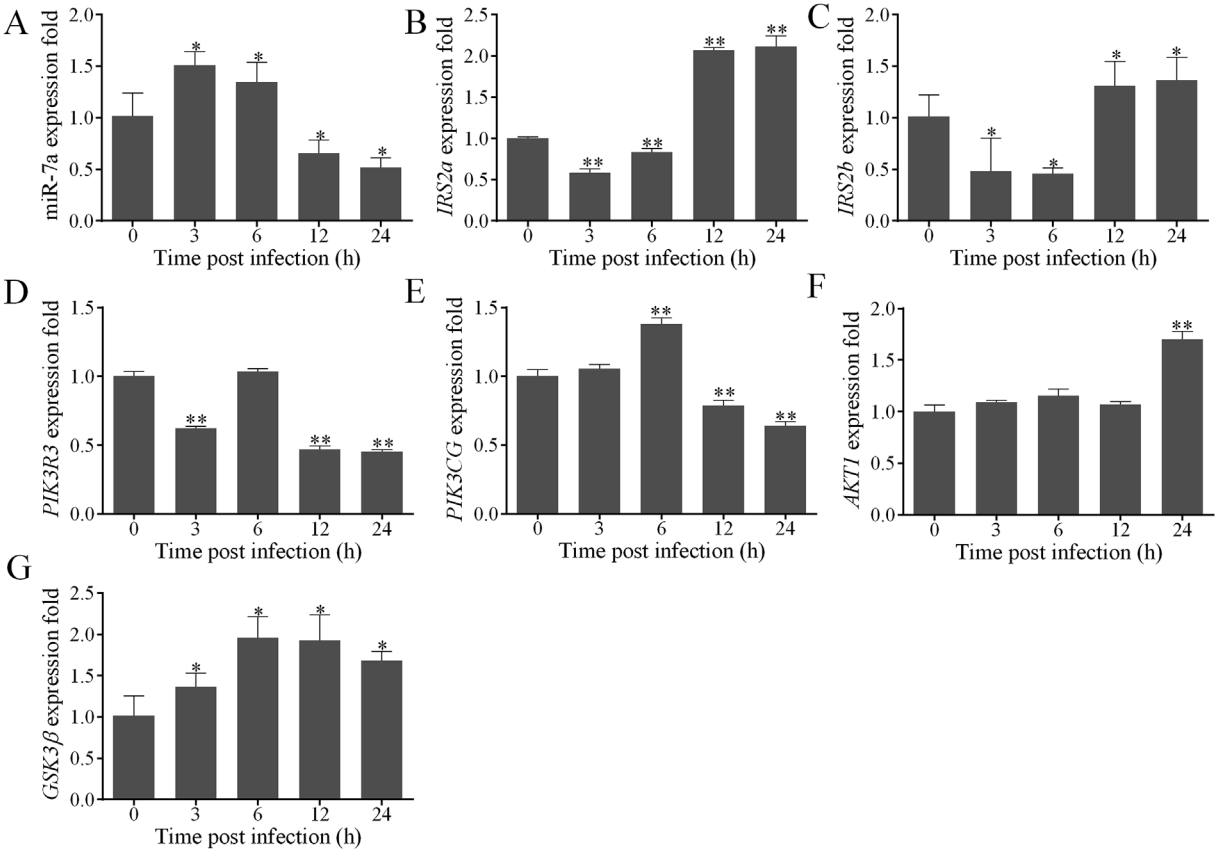

Fig. 5. Upregulated miR-7a inhibits IRS2(s)-mediated PI3K/AKT/GSK3β signaling upon LPS infected primary liver cells. The expression profiles of (A) miR-7a, (B) *IRS2a*, (C) *IRS2b*, (D) *PIK3R3*, (E) *PIK3CG*, (F) *AKT1*, and (G) *GSK3β* at various times post-infection. **, $P < 0.01$; *, $P < 0.05$ versus the controls.

regulatory relationship between DE miRNAs and their predicted target genes, the mimics of 8 miRNAs were synthesized, and 21 target reporter plasmids (pmirGLO-gene-3′UTRs) were constructed which contained a firefly luciferase reporter linked to the 3′UTRs of the target mRNAs. A total of 22 miRNA-mRNA pairs were examined by co-transfection with miRNA mimics and their potential target reporter plasmids in HEK-293T cells. The results showed that luciferase activity was significantly reduced in cells co-transfected with miR-7a mimic and pmirGLO-IRS2a-3′UTR or pmirGLO-IRS2b-3′UTR (Fig. 2).

3.5. IRS2a and IRS2b were novel targets of miR-7a

To further validate the predicted regulatory relationship between 3′UTR of *IRS2*(s) and miR-7a, two reporter plasmids containing the putative binding and mutation sites of miR-7a, namely pmirGLO-IRS2(s)-WT and pmirGLO-IRS2(s)-MT, were constructed and used in dual-luciferase reporter assays in HEK-293T cells. Detail sequences information regarding the binding and mutant sites of miR-7a in the 3′UTR of *IRS2a* and *IRS2b* was shown in Fig. 3A and B. A significant reduction in luciferase activity was detected after the co-transfection with pmirGLO-IRS2(s)-WT and miRNA mimics. But no significant change was observed after co-transfection with pmirGLO-IRS2(s)-MT and miR-7a mimics (Fig. 3C). Therefore, we validated miR-7a negatively regulated *IRS2a* and *IRS2b* by binding to 3′UTR.

3.6. Upregulated miR-7a inhibits PI3K/AKT/GSK3β signaling by targeting IRS2a and IRS2b

To furher clarify whether miR-7a was involved in PI3K/AKT/GSK3β pathway, the expression of miR-7a, *IRS2*(s) and components of PI3K/AKT/GSK3β pathway were analyzed by qRT-PCR.

After infection with *E. tarda in vivo*, the expression of miR-7a was significantly increased at 8 and 24 h post infection (hpi) (Fig. 4A). The expression of *IRS2a* was significantly decreased at 8, 12, 24, and 48 hpi (Fig. 4B) and similar expression profile was detected in *IRS2b* (Fig. 4C). Due to PI3Ks containing many isoforms [25] and antibody is restrict to our studes, *PIK3R3*, *PIK3CG*, and *PIK3CD* were selected for testing by qRT-PCR. The results demonstrated that the expression of *PIK3R3*, *PIK3CG*, and *PIK3CD* showed a similar decreased trend (Fig. 4D–F). The expression of *AKT1* was only decreased at 3 hpi (Fig. 4G). And the expression of *GSK3β* was significantly increased at 3, 8, 24, and 48 hpi (Fig. 4H).

In vitro, primary liver cells were treated with LPS and the expression profiles were investigated. Results showed that the expression of miR-7a was increased at 3 and 6 hpi, while decreased at 12 and 24 hpi (Fig. 5A). Conversely, the expression of *IRS2a* and *IRS2b* decreased at 3 and 6 hpi and increased at 12 and 24 hpi (Fig. 5B and C). The expression of *PIK3R3* and *PIK3CG* were decreased (Fig. 5D and E), while no expression of *PIK3CD* was detected. As shown in Fig. 5F, the decreased trend of *AKT1* expression was not detected. And the expression of *GSK3β* was significantly increased after stimulation with LPS (Fig. 5G).

Furthermore, we treated HKLs with LPS *in vitro*. The expression of miR-7a was significantly increased after stimulation with LPS (Fig. 6A). Conversely, the expression of *IRS2a* and *IRS2b* were decreased (Fig. 6B and C). The expression of *PIK3R3* and *PIK3CD* were decreased (Fig. 6D–E), while no distinct difference was detected in expression of *PIK3CD* (Fig. 6F). The expression of *AKT1* was significantly decreased after stimulation with LPS (Fig. 6G). And the expression of *GSK3β* was increased at 6 and 12 hpi (Fig. 6H). Therefore, these results showed that increased miR-7a might inhibit PI3K/AKT/GSK3β signaling by targeting *IRS2a* and *IRS2b*.

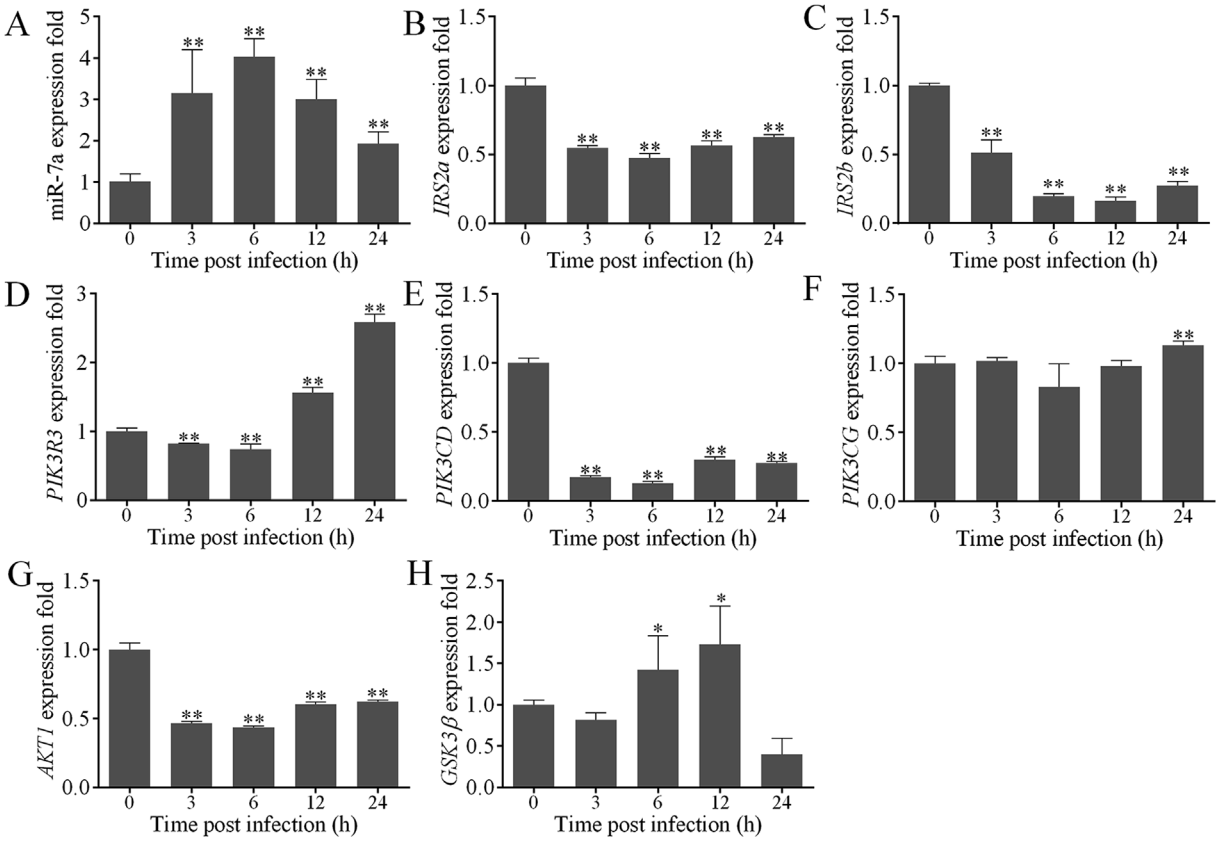

Fig. 6. Upregulated miR-7a inhibits IRS2(s)-mediated PI3K/AKT/GSK3β signaling upon LPS infected HKLs. The expression profiles of (A) miR-7a, (B) *IRS2a*, (C) *IRS2b*, (D) *PIK3R3*, (E) *PIK3CD*, (F) *PIK3CG*, (G) *AKT1*, and (H) *GSK3β* at various times post-infection. **, $P < 0.01$; *, $P < 0.05$ versus the controls.

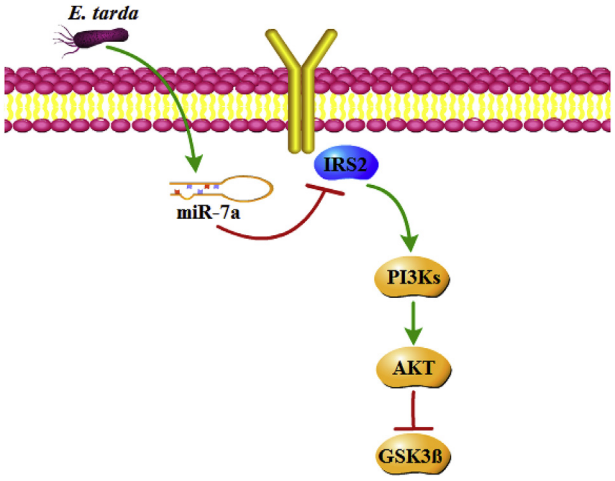

Fig. 7. Schematic representation of the involvement of miR-7a in the host-pathogen interaction by targeting *IRS2a* and *IRS2b* in Japanese flounder.

4. Discussion

As an important post-transcriptional regulator, increasing evidences have demonstrated that miRNAs can regulate host immune responses in mammals, whereas it is rare know the underlying immunoregulatory mechanisms of miRNAs in teleost. Japanese flounder is an economically important marine fish with in-depth research from transcriptome [26], whole-genome [27], to immune genes [28], which is an excellent model for studying the immune response of teleost.

To study immunoregulatory function of miRNAs in Japanese flounder, small RNA libraries were constructed and sequenced. According to our deep sequencing approach, 164 conserved mature miRNAs and 193 candidate novel miRNAs were identified. After pairwise comparisons, 17 DE miRNAs were identified after *E. tarda* infection. In this study, our focus was mainly fixed on the DE miRNAs that might be helpful for us to understand the immune responses to *E. tarda* infection in Japanese flounder.

Compared to 4 DE miRNAs at 3 hpi, the number of that increased at 24 hpi. This was consistent with the results of Najib et al. [1] in which the DE miRNAs were increased at 24 hpi compared to 6 and 12 hpi in Japanese flounder infected with viral hemorrhagic septicemia virus (VHSV). It might indicate that the changes of miRNA expressions were progressively related to pathogen infection process. However, the DE miRNAs which showed different expression in challenge group may not directly involved in regulation of immune response, which was also likely to response for maintenance in cell homeostasis during infection. Therefore, further studies were need to verify regulation of DE miRNAs in immune response.

In mammals, miR-7a is an widely studied miRNA and extensive studies have shown that it functions as a tumor suppressor in a variety of tumor cells, including breast cancer [29], lung cancer [30], and hepatocellular carcinoma [31]. miR-7 can modulate PTEN/PI3K/AKT signaling pathway in Gastric cancer cells by suppressing PI3K expression levels [32]. *IRS2* inhibition by miR-7 also reduces activity of PI3K/AKT signaling pathway in melanoma cells [33]. These reports indicate that miR-7a plays an important role in oncology and can regulate the PI3K/AKT signaling pathway by reducing different targets. However, the roles of miR-7a in teleost still remain unknown.

In our studies, it was found that the expression of miR-7a was significantly upregulated in pathogen-challenged individuals and LPS-exposed cells, which hinted that miR-7a was involved in immune response. The function of the miRNAs responding to infection depended on the target gene(s) they regulated. Hence, the best way to understand

the function of miR-7a was to study the function of its target genes. Using dual-luciferase reporter assays, we detected 22 miRNA-mRNA pairs in HEK-293T cells and then the negative regulation of *IRS2a* and *IRS2b* by miR-7a were validated in Japanese flounder.

As a member of the IRS (insulin receptor substrate) family, IRS2 can interact with -SH2 domain containing proteins mainly PI3K [34]. In mammals, subsets of miRNAs have been identified to regulate the PI3K/AKT signaling pathway by directly suppressing *IRS2* expression, such as, miR-106a* [35], miR-551a [36], and miR-766 [37]. Our studies showed that the *E. tarda* and LPS significantly decreased *IRS2a* and *IRS2b* expression *in vivo* and *in vitro*, which suggested an inverse relationship between miR-7a and *IRS2*(s) expression. Thus, *IRS2a* and *IRS2b* could be regulated through miR-7a at the post-transcriptional level. However, further works of overexpression and inhibition of miR-7a were needed for exploring the gene expression levels of *IRS2a* and *IRS2b* to confirm this relationship between miR-7a and *IRS2*(s).

As stated above, both miR-7a and *IRS2* can mediate the PI3K/AKT signaling pathway in mammals. Inhibition of IRS2 by miR-7a would reduce the signaling cascade that transmited through PI3K and AKT. We, therefore, sought to evaluate the down-regulation of PI3K/AKT signaling components in pathogen-challenged individuals and LPS-exposed cells. Several miRNAs have been reported to directly target *PIK3R3* [38], *PIK3CD* [39], and *PI3KCG* [40] to attenuate PI3K/AKT pathway. Therefore, we detected their expressions. The results showed that mRNA expression of *PIK3R3*, *PIK3CD*, and *PI3KCG* were inhibited in pathogen-challenged individuals and LPS-exposed cells. Frequently, immunoblot for AKT phosphorylated at Ser^{473} was used as a surrogate marker for AKT activity. Due to absence of specific antibody in *P.olivaceus*, we only test AKT mRNA expression. The AKT1, one of AKT isoforms, is ubiquitously expressed to high levels in the cytoplasm, whereas expression of the other two isoforms is localized to certain tissues and subcellular loci [41]. Due to the relatively global role of AKT1 in regulation of PI3K/AKT signaling pathway, we detected AKT1 mRNA expression. The mRNA expression significantly attenuated in LPS-treated HKLs, while there was no significant change in pathogen-challenged individuals and LPS-treated primary liver cells. To some extent, these results may suggest the reduction of PI3K/AKT signaling cascade in pathogen-challenged individuals and LPS-exposed cells. GSK3β, a key downstream effector molecule of PI3K pathway, plays an important role in different signal transduction pathways of the immune system [42]. In our study, the upregulation of *GSK3β* mRNA expression was detected in pathogen-challenged individuals and LPS-exposed cells, which may suggest that miR-7a acted as an immunoregulatory gene by indirectly increasing *GSK3β* mRNA expression in Japanese flounder.

By large scale miRNA profiling using deep sequencing, we identified the miRNAome of Japanese flounder liver followed by quantitative analysis to validate those miRNAs that were DE miRNAs in the challenge group. We had obtained large number of putative target genes by use of *in silico* methods. And miR-7a had been further investigated by studying its effect on target genes (*IRS2a* and *IRS2b*) and PI3K/AKT signaling. However, furher studies were need to investigate the effect on IRS2-mediated PI3K/AKT signaling when the expression of miR-7a was increased or suppressed *in vivo* and *in vitro*.

In conclusion, the present study revealed that miR-7a in Japanese flounder showed significantly increased in pathogen-challenged individuals and LPS-exposed cells. *IRS2a* and *IRS2b* were considered two novel targets of miR-7a, which were confirmed by dual-luciferase reporter assays. Based on our findings, we indicated that miR-7a was maybe a new negative regulator of IRS2-mediated PI3K/AKT/GSK3β signaling pathway (Fig. 7). Studies on miR-7a would enrich knowledge of its functions in immunoregulatory mechanism in teleost.

Conflicts of interest

We declare that we have no financial and personal relationships with other people or organizations.

Acknowledgements

This work was supported by National Natural Science Foundation of China (No. 31802327).

Appendix A. Supplementary data

Supplementary data to this article can be found online at https://doi.org/10.1016/j.fsi.2019.03.076.

References

[1] A. Najib, M.S. Kim, S.H. Choi, Y.J. Kang, K.H. Kim, Changes in microRNAs expression profile of olive flounder (*Paralichthys olivaceus*) in response to viral hemorrhagic septicemia virus (VHSV) infection, Fish Shellfish Immunol. 51 (2016) 384–391.
[2] Z. Sha, G. Gong, S. Wang, Y. Lu, L. Wang, Q. Wang, et al., Identification and characterization of *Cynoglossus semilaevis* microRNA response to *Vibrio anguillarum* infection through high-throughput sequencing, Dev. Comp. Immunol. 44 (2014) 59–69.
[3] S.B. Park, T. Aoki, T.S. Jung, Pathogenesis of and strategies for preventing *Edwardsiella tarda* infection in fish, Vet. Res. 43 (2012) 67.
[4] J.M. Janda, S.L. Abbott, Infections associated with the genus Edwardsiella: the role of *Edwardsiella tarda* in human disease, Clin. Infect. Dis. : Off. Publ. Infec. Dis. Soc. Amer. 17 (1993) 742–748.
[5] B.R. Mohanty, P.K. Sahoo, Edwardsiellosis in fish: a brief review, J. Biosci. 32 (2007) 1331–1344.
[6] D.P. Bartel, MicroRNAs: genomics, biogenesis, mechanism, and function, Cell 116 (2004) 281–297.
[7] J.C. Carrington, V. Ambros, Role of MicroRNAs in plant and animal development, Science (New York, NY) 301 (2003) 336–338.
[8] I.W. Boss, R. Renne, Viral miRNAs and immune evasion, Biochimica et Biophysica Acta (BBA) - Gene Regulatory Mechanisms, vol. 1809, 2011, pp. 708–714.
[9] R.M. O'Connell, D.S. Rao, A.A. Chaudhuri, D. Baltimore, Physiological and pathological roles for microRNAs in the immune system, Nat. Rev. Immunol. 10 (2010) 111.
[10] X-l Guan, B-c Zhang, L. Sun, pol-miR-194a of Japanese flounder (*Paralichthys olivaceus*) suppresses type I interferon response and facilitates *Edwardsiella tarda* infection, Fish Shellfish Immunol. 87 (2019) 220–225.
[11] Y.-H. Hu, B.-C. Zhang, H.-Z. Zhou, X.-L. Guan, L. Sun, *Edwardsiella tarda*-induced miRNAs in a teleost host: global profile and role in bacterial infection as revealed by integrative miRNA-mRNA analysis, Virulence 8 (2017) 1457–1464.
[12] J. Han, Y. Sun, W. Song, T. Xu, microRNA-145 regulates the RLR signaling pathway in miiuy croaker after poly(I:C) stimulation via targeting MDA5, Dev. Comp. Immunol. 68 (2017) 79–86.
[13] B-c Zhang, Z-j Zhou, L. Sun, pol-miR-731, a teleost miRNA upregulated by megalocytivirus, negatively regulates virus-induced type I interferon response, apoptosis, and cell cycle arrest, Sci. Rep. 6 (2016) 28354.
[14] D. Bi, J. Cui, Q. Chu, T. Xu, MicroRNA-21 contributes to suppress cytokines production by targeting TLR28 in teleost fish, Mol. Immunol. 83 (2017) 107–114.
[15] S. Ni, Y. Yu, J. Wei, L. Zhou, S. Wei, Y. Yan, et al., MicroRNA-146a promotes red spotted grouper nervous necrosis virus (RGNNV) replication by targeting TRAF6 in orange spotted grouper, *Epinephelus coioides*, Fish Shellfish Immunol. 72 (2018) 9–13.
[16] Y. Tan, J. Zheng, S. Tung, I. Rosenshine, K. Leung, Role of type III secretion in *Edwardsiella tarda* virulence, Microbiology 151 (2005) 2301–2313.
[17] Z. Li, X. Liu, J. Liu, K. Zhang, H. Yu, Y. He, et al., Transcriptome profiling based on protein–protein interaction networks provides a core set of genes for understanding blood immune response mechanisms against *Edwardsiella tarda* infection in Japanese flounder (*Paralichthys olivaceus*), Dev. Comp. Immunol. 78 (2017) 100–113.
[18] X. Liu, Z. Li, W. Wu, Y. Liu, J. Liu, Y. He, et al., Sequencing-based network analysis provides a core set of gene resource for understanding kidney immune response against *Edwardsiella tarda* infection in Japanese flounder, Fish Shellfish Immunol. 67 (2017) 643–654.
[19] M.R. Friedländer, S.D. Mackowiak, N. Li, W. Chen, N. Rajewsky, miRDeep2 accurately identifies known and hundreds of novel microRNA genes in seven animal clades, Nucleic Acids Res. 40 (2011) 37–52.
[20] A.J. Enright, B. John, U. Gaul, T. Tuschl, C. Sander, D.S. Marks, MicroRNA targets in Drosophila, Genome Biol. 5 (2003) R1.
[21] K.C. Miranda, T. Huynh, Y. Tay, Y.-S. Ang, W.-L. Tam, A.M. Thomson, et al., A pattern-based method for the identification of MicroRNA binding sites and their corresponding heteroduplexes, Cell 126 (2006) 1203–1217.
[22] D.W. Huang, B.T. Sherman, R.A. Lempicki, Bioinformatics enrichment tools: paths toward the comprehensive functional analysis of large gene lists, Nucleic Acids Res. 37 (2009) 1–13.
[23] S. Dutta, B. Sinha, B. Bhattacharya, B. Chatterjee, S. Mazumder, Characterization of a galactose binding serum lectin from the Indian catfish, Clarias batrachus: possible involvement of fish lectins in differential recognition of pathogens, Comp. Biochem. Physiol. C Toxicol. Pharmacol. 141 (2005) 76–84.
[24] R. Andreassen, M.M. Worren, B. Høyheim, Discovery and characterization of miRNA genes in atlantic salmon (*Salmo salar*) by use of a deep sequencing

approach, BMC Genomics 14 (2013) 482.
[25] P.T. Hawkins, L.R. Stephens, PI3K signalling in inflammation, Biochim. Biophys. Acta Mol. Cell Biol. Lipids 1851 (2015) 882–897.
[26] Z. Li, X. Liu, J. Cheng, Y. He, X. Wang, Z. Wang, et al., Transcriptome profiling provides gene resources for understanding gill immune responses in Japanese flounder (*Paralichthys olivaceus*) challenged with *Edwardsiella tarda*, Fish Shellfish Immunol. 72 (2018) 593–603.
[27] C. Shao, B. Bao, Z. Xie, X. Chen, B. Li, X. Jia, et al., The genome and transcriptome of Japanese flounder provide insights into flatfish asymmetry, Nat. Genet. 49 (2017) 119–124.
[28] J. Liu, D. Cao, Y. Liu, Z. Li, Y. Si, Z. Wang, et al., Expression and functional analysis of receptor-interacting serine/threonine kinase 2 (RIP2) in Japanese flounder (*Paralichthys olivaceus*), Fish Shellfish Immunol. 75 (2018) 327–335.
[29] Y. Shi, X. Luo, P. Li, J. Tan, X. Wang, T. Xiang, et al., miR-7-5p suppresses cell proliferation and induces apoptosis of breast cancer cells mainly by targeting REGγ, Cancer Lett. 358 (2015) 27–36.
[30] H. Liu, X. Wu, J. Huang, J. Peng, L. Guo, miR-7 modulates chemoresistance of small cell lung cancer by repressing MRP1/ABCC1, Int. J. Exp. Pathol. 96 (2015) 240–247.
[31] F. Wang, Y. Qiang, L. Zhu, Y. Jiang, Y. Wang, X. Shao, et al., MicroRNA-7 down-regulates the oncogene VDAC1 to influence hepatocellular carcinoma proliferation and metastasis, Tumor Biol. 37 (2016) 10235–10246.
[32] H. Pan, T. Li, Y. Jiang, C. Pan, Y. Ding, Z. Huang, et al., Overexpression of circular RNA ciRS-7 abrogates the tumor suppressive effect of mir-7 on gastric cancer via PTEN/PI3K/AKT signaling pathway, J. Cell. Biochem. 119 (2018) 440–446.
[33] K.M. Giles, R.A.M. Brown, M.R. Epis, F.C. Kalinowski, P.J. Leedman, miRNA-7-5p inhibits melanoma cell migration and invasion, Biochem. Biophys. Res. Commun. 430 (2013) 706–710.
[34] G. Sesti, M. Federici, M.L. Hribal, D. Lauro, P. Sbraccia, R. Lauro, Defects of the insulin receptor substrate (IRS) system in human metabolic disorders, FASEB J. 15 (2001) 2099–2111.
[35] Y. Ma, H. Zhang, X. He, H. Song, Y. Qiang, Y. Li, et al., miR-106a* inhibits the proliferation of renal carcinoma cells by targeting IRS-2, Tumor Biol. 36 (2015) 8389–8398.
[36] Z. Du, X. Sha, Demethoxycurcumin inhibited human epithelia ovarian cancer cells' growth via up-regulating miR-551a, Tumour biology : the Journal of the International Society for Oncodevelopmental Biology and Medicine, vol. 39, 2017 1010428317694302.
[37] J. Zhao, Z. Li, Y. Chen, S. Zhang, L. Guo, B. Gao, et al., MicroRNA766 inhibits papillary thyroid cancer progression by directly targeting insulin receptor substrate 2 and regulating the PI3K/Akt pathway, Int. J. Oncol. 54 (2019) 315–325.
[38] G. Cao, W. Dong, X. Meng, H. Liu, H. Liao, S. Liu, MiR-511 inhibits growth and metastasis of human hepatocellular carcinoma cells by targeting PIK3R3, Tumor Biol. 36 (2015) 4453–4459.
[39] Y. Fang, J.-L. Xue, Q. Shen, J. Chen, L. Tian, MicroRNA-7 inhibits tumor growth and metastasis by targeting the phosphoinositide 3-kinase/Akt pathway in hepatocellular carcinoma, Hepatology 55 (2012) 1852–1862.
[40] S. Chen, F. Li, H. Chai, X. Tao, H. Wang, A. Ji, miR-502 inhibits cell proliferation and tumor growth in hepatocellular carcinoma through suppressing phosphoinositide 3-kinase catalytic subunit gamma, Biochem. Biophys. Res. Commun. 464 (2015) 500–505.
[41] T.F. Franke, PI3K/Akt: getting it right matters, Oncogene 27 (2008) 6473.
[42] H. Wang, J. Brown, M. Martin, Glycogen synthase kinase 3: a point of convergence for the host inflammatory response, Cytokine 53 (2011) 130–140.